Synthesis of Gold Nanoshells with Plasmon Resonance tuned to the Infrared Region of the Electromagnetic Spectrum

R. RUVALCABA-ONTIVEROS, H. ESPARZA-PONCE, A. CARRASCO-HERNANDEZ, C.D. GÓMEZ-ESPARZA, E. ORRANTIA-BORUNDA, J. G. MURILLO-RAMIREZ
Centro de Investigación en Materiales Avanzados, S.C.
Miguel de Cervantes Saavedra 120 Chihuahua, Chih., C.P. 31136.
MEXICO

A. DUARTE-MOLLER*
Universidad De La Salle Bajío
Av. Universidad 602, Lomas del Campestre, León Guanajuato, 37150, MEXICO

J.M. OLIVARES-RAMIREZ,
Universidad Tecnológica de San Juan del Río.
Av. La Palma No. 125, Col. Vista Hermosa, San Juan del Río, Qro. C.P. 76800. MEXICO
*jduarte@delasalle.edu.mx

Abstract: Gold nanoshells (GNS) present a silica core surrounded by a gold shell, present a shift on their surface plasmon resonance (SPR) to the near-infrared (NIR) part of the electromagnetic spectrum, when synthesized with specific dimensions. This paper presents a simple method to prepare the nanoshells, a step by step characterization, as well as their absorbance spectrum. For the synthesis, silica spheres, with approximately 130 ± 5 nm in diameter, were prepared using the Stöber method and then functionalized with 3-aminopropyltriethoxysilane (APTES). The gold nanoparticles (GNPs), with a diameter of 7 ± 3 nm, were produced by the reduction of chloroauric acid. Then, the silica was seeded with the GNPs to later grow a gold shell with the help of $Au(OH)_4^-$ ions and formaldehyde. UV-Vis spectroscopy results showed a progressive shift on the absorbance peak to the NIR throughout the synthesis. Transmission electron microscope (TEM) and scanning electron microscope (SEM) images suggest that the absorption peak movement coincided with the completion of the shell. Furthermore, when the sample was irradiated with an 820nm wavelength/3.1 mW laser, its temperatures increased 6.3 °C in 2 minutes, showing its absorbance in the NIR.

Key words: Gold nanoshells, surface plasmon resonance, near infrared, gold nanoparticles, absorption, silica.

1. Introduction

There are hundreds of types of cancer, and each one has different characteristics [1]. Therefore, science utilizes the most innovative discoveries to find new treatments, and nanotechnology offers a wide variety of options. One example of this is the nanoparticle colloids, they can be designed to concentrate on specific organs, passive targeting, or their surfaces can be modified by an antibody or ligand to get attached to a specific target, active targeting [2]. Furthermore, metallic nanoparticles, like GNS, present interesting optical properties. Their SPR shifts their absorption to the NIR region when they are synthesized with specific geometry and dimensions [3]. This shift offers a great potential for applications in the medical field because GNPs are bio-inert [4], and the cytotoxicity of the silica has been widely studied [5]. Additionally, the wavelengths of the NIR spectrum are considered the optical window of the human body. As a result, while most biological soft tissues have low absorption of these wavelengths [6], GNS absorb them causing them to increase their temperature. Some applications are the photothermal therapy [7], optical imaging [8], drug release [9], as well as providing a near instantaneous in situ whole blood assay [10]. The synthesis of the GNS has been extensively explored, but on this paper, we present a simple and effective method of preparation that shortens the time of the traditional procedures published before. The reductions of the time were obtained by, first modifying the Stöber method of synthesis of silica particles, and obtaining samples at 30, 60, 90 and 120 minutes throughout the reaction. Also, during the seeding process, where the silica is decorated with GNPs, a sample was obtained using only 30 minutes of resting time and compared with another one with the full 2 hrs of the resting time previously suggested. In both cases, SEM images were obtained showing that 30 minutes were enough to accomplish the complete reactions. In consequence, the total time of the process was reduced by 3 hrs.

2. Experimental

2.1 Materials

Ethanol (100%), tetraethyl orthosilicate (TEOS) (98%), 3-aminopropyltriethoxysilane (APTES) (99%), trisodium citrate dihydrate, Gold (III) chloride trihydrate ($HAuCl_4$, 49%), formaldehyde (37%), and sodium borohydride ($NaBH_4$, 98 %) were purchased from Sigma-Aldrich. Potassium carbonate (K_2CO_3, 99%) and ammonium hydroxide (28%), were purchased from J.T. Baker. All the solutions were prepared with deionized water.

2.2 Preparation of silica spheres

Silica particles were prepared by modifying the Stöber method [11]. 50 ml of ethanol, 2.5 ml of deionized water, 4.25 ml of ammonium hydroxide were stirred for 5 min. Then, 0.75 ml of TEOS was added dropwise. The solution was heated at 40°C. Temperature and agitation were kept for 2 hrs. The color of the solution changed from transparent to opaque white approximately 10 min after adding the TEOS. Samples were obtained at 30, 60, 90 and 120 min of adding the TEOS to observe the evolution of the process.

2.3 Functionalization of the silica spheres

In order to create open links over the silica to attach the GNPs, the silica was functionalized with APTES on a 1:1 silica:APTES volume ratio. The solution was stirred for 5 min and left still overnight at room temperature. The functionalized silica particles precipitated in the solution. They were centrifuged and washed in deionized water 3 times and dispersed in deionized water.

2.4 Synthesis of Gold Nanoparticles

The method presented by Abdollahi et al [13] was followed to elaborate the GNPs. 1 ml of 1% $HAuCl_4$ solution, 2 ml of 1% trisodium citrate and 1 ml of fresh 0.075% $NaBH_4$ in 1% trisodium citrate were added into 100 ml of deionized water at room temperature, stirred for 10 min and used immediately after.

2.5 Synthesis of Gold Nanoshells

For the seeding process, 100 ml of GNPs and 10 ml of functionalized silica were stirred for 5 min and left standing for 2 hrs. The solution was centrifuged and washed in deionized water 3 times. Finally, it was sonicated in 10 ml of deionized water. The same procedure was followed but the solution was left still for only 30 min to observe the development of the GNS through time.

For the shell growth process, a K-Au solution was prepared by mixing 100 ml of 2mM K_2CO_3 solution and 1.5 ml of 1% $HAuCl_4$ for 30 min. The color of the solution changed from light yellow to transparent. It was left still overnight at room temperature in an amber glass bottle to facilitate the formation of $Au(OH)_4^-$ ions. Then, 100 ml of K-Au solution and 5 ml of seeded silica were stirred for 5 min. Next, 5 ml of formaldehyde were added to the solution and stirred for 10 min. The solution was left still for 50 min. Finally, it was centrifuged, washed and dispersed in 10 ml of deionized water.

2.6 Characterization

Images were obtained using the Field Emission Scanning Electron Microscope JEOL JSM-7401F (SEM 7401), the Transition Electron Microscope HT7700 Hitachi (TEM) and the Scanning Electron Microscope JEOL JSM5800LV (SEM 5800). For the UV-Vis spectra, the Evolution 220 Spectrophotometer UV-Vis Thermo Scientific was used. The FTIR spectra were obtained with an IRAffinity-1S Fourier Transform Infrared Spectrophotometer Shimadzu. The sample was irradiated with an 820nm wavelength/3.1 mW laser Thorlabs Multi-channel Fiber Coupled Laser Source, and the infrared images were taken with a TrueIR Agilent keysight U5855A. Measurement of the particles and histograms were acquired with the Image J® software [12].

3. Results and discussion

3.1 Characterization of the silica particles

Fig. 1 presents images of silica particles taken at different moments of the reaction showing that after 30 min, the process is complete, and the particles do not present any significant change. Additionally, the images were studied with the software Image J® to calculate the particle size distribution. Over 220 particles from different areas of the sample were counted and measured to obtain the histograms. The information on Fig. 2 illustrates that the average diameter of the spheres at different reaction times is approximately the same.

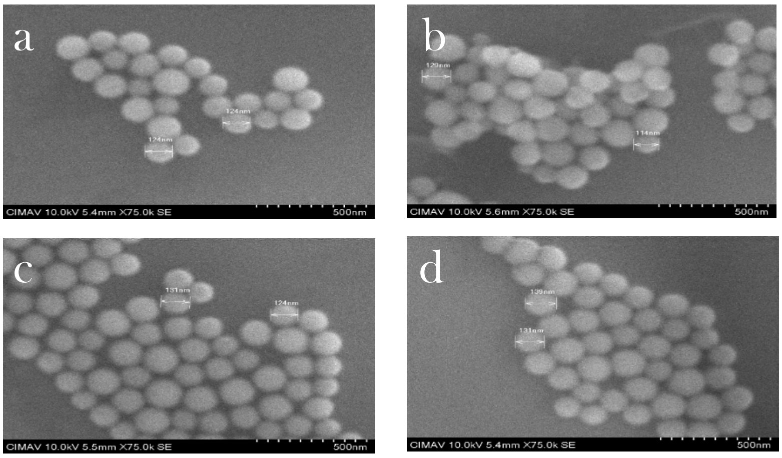

Fig. 1: SEM 5800 images of Silica particles at a)30, b)60, c)90 and d)120

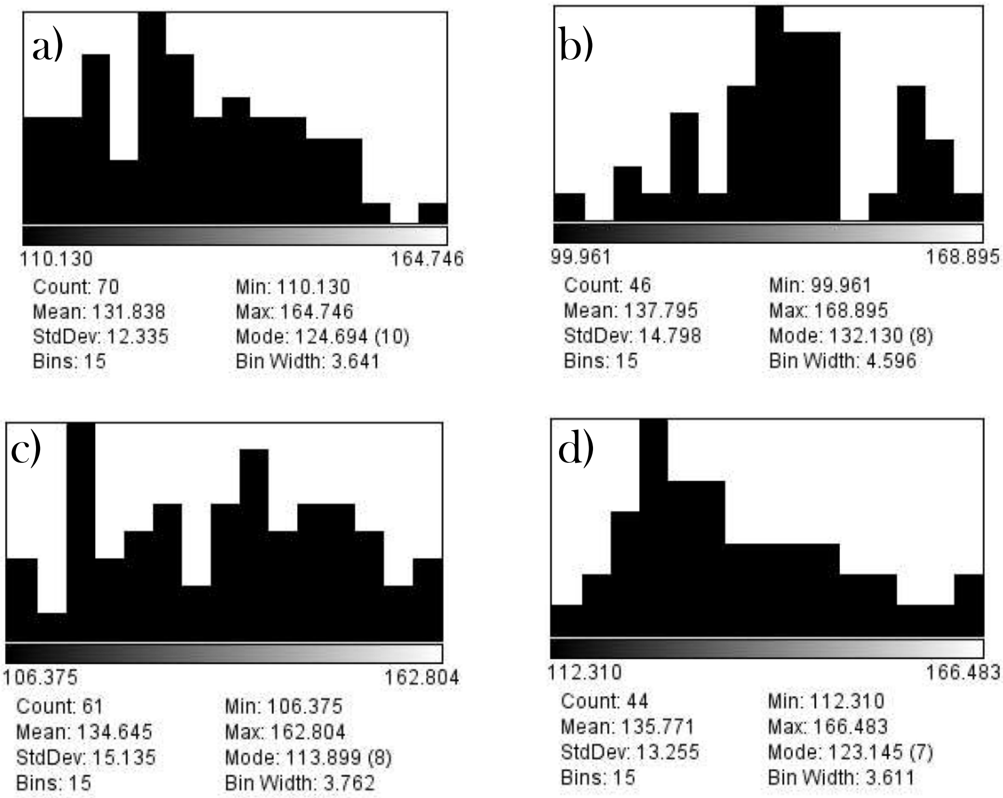

Fig. 2: Histograms of the diameter distribution of the silica particles at a)30, b)60, c)90 and d)120 min throughout the synthesis.

Therefore, a reaction time of more than 30 min does not result in a significant change in the sample. As a result, the total process time can be reduced by 1 hour and 30 min when compared with similar works where the synthesis time is at least 2 hrs [13,14,15,16].

3.2 Characterization of the functionalized silica spheres

The functionalization of the silica with a primary amine group ($-NH_2$) was accomplished using APTES which changes the superficial charge providing an electrostatic link for the GNPs to attach [17]. This superficial modification was verified by the FTIR spectrum shown in Fig. 3 where the vibrations of primary amines are found between 3550-3330 cm^{-1} which correspond to the vibrations of a primary amine group [18].

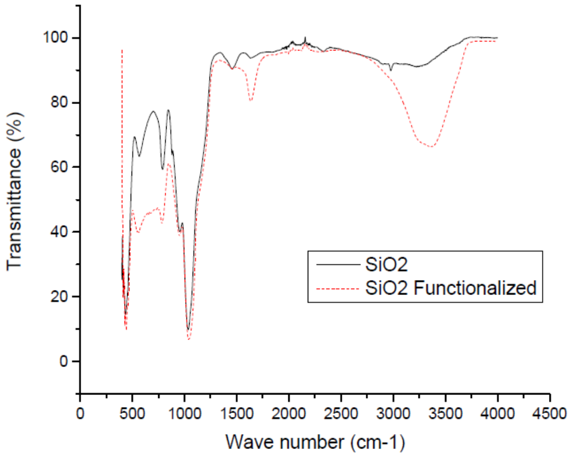

Fig. 4: FTIR spectrum of silica and silica functionalized

3.3 Characterization of GNPs

Fig. 4 illustrates the synthesized GNPs with a diameter of 7±3 nm and spherical shape overall. This GNPs were used immediately after their synthesis to avoid the agglomeration of the nanoparticles.

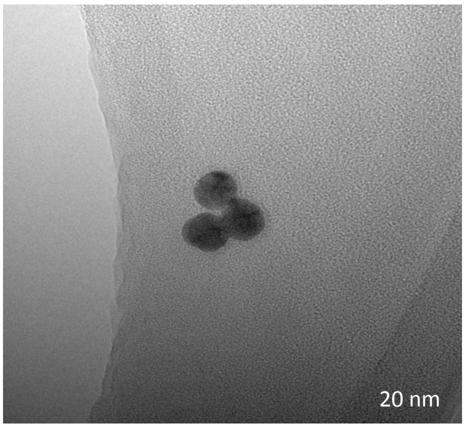

Fig. 5: TEM images of GNPs

3.4 Characterization of seeded silica particles

Fig. 5a presents an SEM image of seeded silica with 30 min of resting time, while Fig. 5 b presents an SEM image of seeded silica with 120 min of resting time. These samples were taken with the purpose of observing the seeding process. Yet, the images show that 30 min is enough time to create the seeds. Both images display approximately the same number of nucleus per silica particle. Even though a complete shell was not formed, the seeds are ready to grow the gold shell on the next step.

Fig. 6 is a TEM image of one silica particle decorated with GNPs with approximately 240 seeds of gold. This image corroborates the seeding process as well as the silica functionalization.

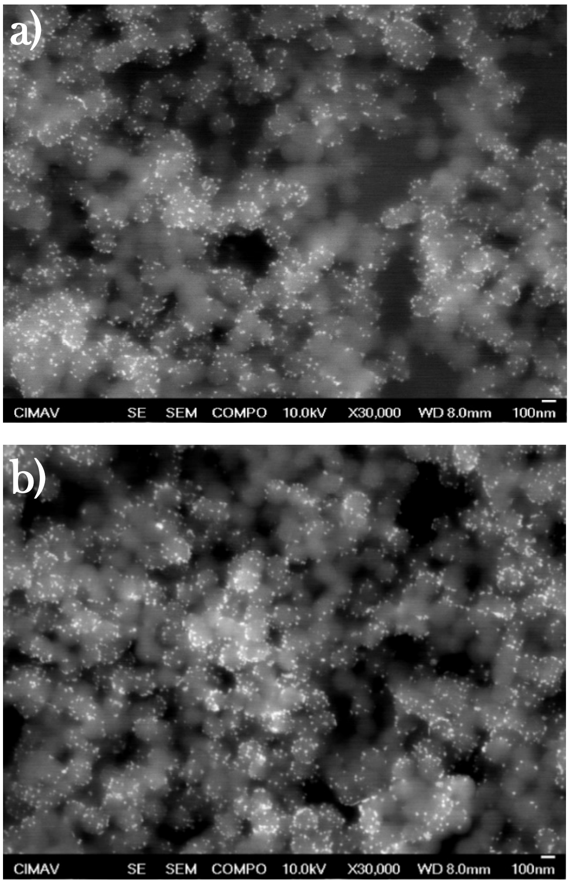

Fig. 3: a) SEM image of seeded silica with 30 min of resting time and b) SEM image of seeded silica with 120 min of resting time

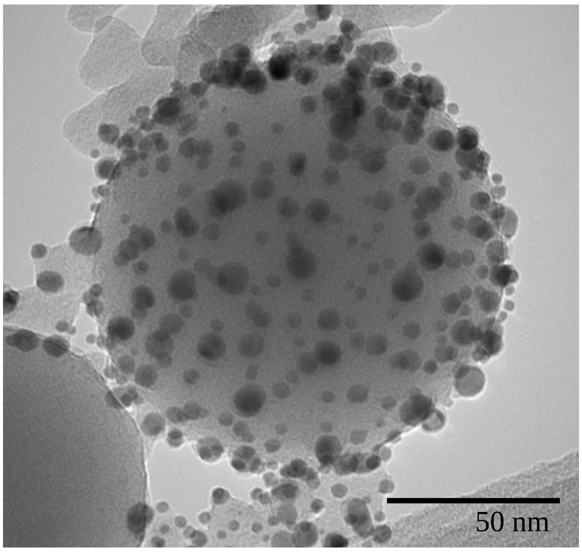

Fig. 6: TEM image of a gold decorated silica particle

3.5 Characterization of gold nanoshells

On Fig. 7a is observed that the silica particles are almost surrounded with gold. The higher density of gold, the separation of the GNPs [19] and the dielectric properties of the silica [3] contribute to the absorption of the NIR wavelength, which causes the increase in temperature. On Fig. 7b a more detailed view of the gold shell can be appreciated. It is important to note that it is not a layer of gold but several GNPs close together.

3.6 UV-Vis spectrum

Fig. 8 presents the UV-Vis spectrum of the particles all through the process. Silica particles, as well as functionalized silica particles, do not show significant absorption on the NIR. As for the GNPs, they exhibit their characteristic absorption between 520-530 nm [20]. However, on the seeded silica particles, it is noticeable the slight shift to the NIR. While on the GNS the peak not only shifted to the NIR, but it kept a high absorbance all the way to 1100 nm. The absorbance of the GNS is due to the SPR that creates an electric field on the surface increasing the absorption of this wavelengths. SPR happens when metal nanoparticles are irradiated with a wavelength bigger than their size, exciting the electrons of the conducting band [3].

3.7 Thermography

To verify the absorbance of the GNS, they were irradiated with an 852nm laser with a power of 3.1mW. Fig. 9a displays a thermography image of the sample before irradiation, meanwhile Fig. 9b *shows* a thermography 2 min after the irradiation started. The sample is located on point S1, which temperature increased from 24.7 °C to 31.0 °C. This confirms that GNS can absorb light from the NIR.

4. Conclusions

Synthesizing GNS by seeding and growing a gold shell over silica spheres with GNPs showed to be an effective method to tune their absorption to the NIR. The SEM and TEM images show the evolution of the process while the absorbance spectrum displays the GNS shifting over the NIR. In addition, the thermography demonstrates the increase in temperature during the infrared laser irradiation. Hence, we obtained a simple technique of producing GNS that can be used for medical applications thanks to the bio-inert GNPs [3] and the widely studied cytotoxicity of the silica [5].

Acknowledgments

We thank Consejo Nacional de Ciencia y Tecnología (CONACyTt) and Centro de Investigacion en Materiales Avanzados (CIMAV) for the financial support, Dr. Jose Guadalupe Murillo Ramirez for his help with the use of 852 nm wavelength laser, Dr. Pedro Piza for lending us the thermographic camera, Ing. Wilber Antunez Flores and M.C. Karla Campos Venegas for helping us obtain the TEM and SEM images.

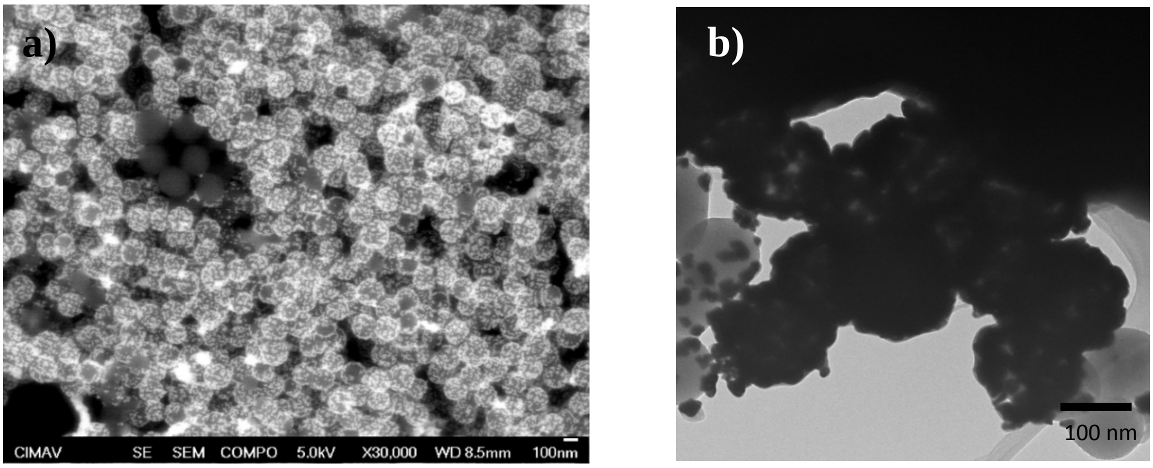

Fig. 7: a) SEM image of GNS and b) TEM image of GNS

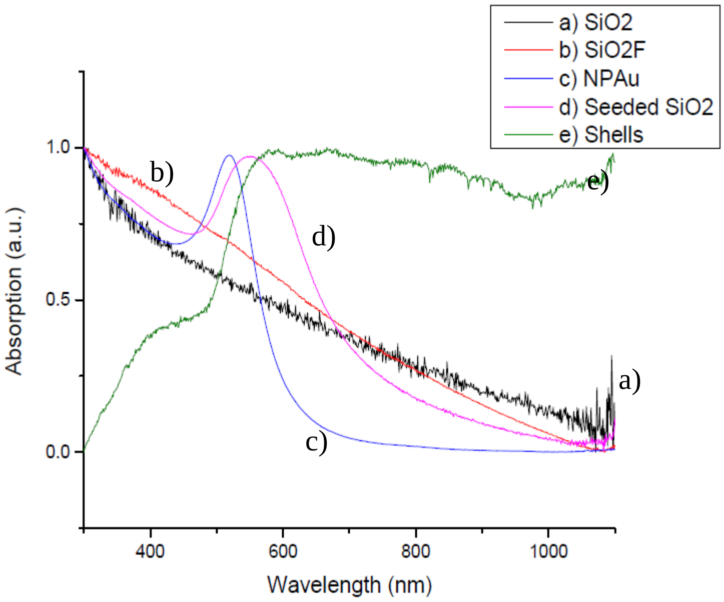

Fig. 8: UV-Vis Spectrum of a) Silica, b) Functionalized silica, c) GNPs, d) Gold seeded silica and e) GNS

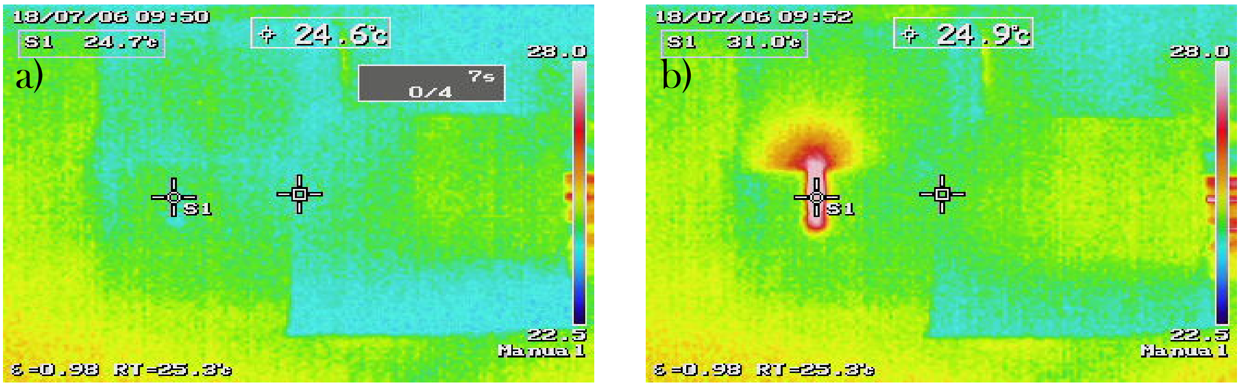

Fig. 9: Thermography images of the GNS taken a) before and b)after being irradiated with 852nm laser

References

[1] "Tipos De Cáncer." National Cancer Institute. N.p., 2018. Web. 19 Nov. 2017.

[2] Pissuwan, Dakrong, Stella M. Valenzuela, and Michael B. Cortie. "Therapeutic Possibilities Of Plasmonically Heated Gold Nanoparticles." Trends in Biotechnology 24.2 (2006): 62-67. Web. 5 Dec. 2017.

[3] Petryayeva, Eleonora, and Ulrich J. Krull. "Localized Surface Plasmon Resonance: Nanostructures, Bioassays And Biosensing—A Review." Analytica Chimica Acta 706.1 (2011): 8-24. Web.

[4] Jenkins, James T. et al. "Excretion And Toxicity Of Gold–Iron Nanoparticles." Nanomedicine: Nanotechnology, Biology and Medicine 9.3 (2013): 356-365. Web.

[5] Spyrogianni, Anastasia et al. "The Effect Of Settling On Cytotoxicity Evaluation Of Sio 2 Nanoparticles." Journal of Aerosol Science 108 (2017): 56-66. Web.

[6] Anderson, R. Rox, and John A. Parrish. "The Optics Of Human Skin." Journal of Investigative Dermatology 77.1 (1981): 13-19. Web.

[7] Wang, Lu et al. "Photothermo-Chemotherapy Of Cancer Employing Drug Leakage-Free Gold Nanoshells." Biomaterials 78 (2016): 40-49. Web.

[8] Tuersun, Paerhatijiang, and Xiang'e Han. "Optimal Design Of Gold Nanoshells For Optical Imaging And Photothermal Therapy." Optik - International Journal for Light and Electron Optics 125.14 (2014): 3702-3706. Web.

[9] Pissuwan, Dakrong, Stella M. Valenzuela, and Michael B. Cortie. "Therapeutic Possibilities Of Plasmonically Heated Gold Nanoparticles." Trends in Biotechnology 24.2 (2006): 62-67. Web.

[10] Hirsch, L. R. et al. "A Whole Blood Immunoassay Using Gold Nanoshells." Analytical Chemistry 75.10 (2003): 2377-2381. Web.

[11] Stöber, Werner, Arthur Fink, and Ernst Bohn. "Controlled Growth Of Monodisperse Silica Spheres In The Micron Size Range." *Journal of Colloid and Interface Science* 26.1 (1968): 62-69.

[12] Rasband, W.S., ImageJ, U. S. National Institutes of Health, Bethesda, Maryland, USA, http://rsb.info.nih.gov/ij/, 1997-2005

[13] Abdollahi, S. Narjes, Malek Naderi, and Ghassem Amoabediny. "Synthesis And Characterization Of Hollow Gold Nanoparticles Using Silica Spheres As Templates." Colloids and Surfaces A: Physicochemical and Engineering Aspects 436 (2013): 1069-1075. Web.

[14] Phonthammachai, Nopphawan et al. "Synthesis Of Contiguous Silica−Gold Core−Shell Structures: Critical Parameters And Processes." Langmuir 24.9 (2008): 5109-5112. Web.

[15] Lee, Sang Ho et al. "Preparation And Characterization Of Polymeric Thin Films Containing Gold Nanoshells Via Electrostatic Layer-By-Layer Self-Assembly." Thin Solid Films 558 (2014): 200-207.

[16] Elbialy, Nihal, Noha Mohamed, and Ahmed Soltan Monem. "Synthesis, Characterization And Application Of Gold Nanoshells Using Mesoporous Silica Core." Microporous and Mesoporous Materials 190 (2014): 197-207. Web.

[17] Wei, Xiang et al. "Plasmonic Nanoshells Enhanced Laser Desorption/Ionization Mass Spectrometry For Detection Of Serum Metabolites." Analytica Chimica Acta 950 (2017): 147-155.

[18] Socrates, G. Infrared Characteristic Group Frequencies. New York: Wiley, 2000. Print.

[19] Huang, Xiaohua, and Mostafa A. El-Sayed. "Gold Nanoparticles: Optical Properties And Implementations In Cancer Diagnosis And Photothermal Therapy." Journal of Advanced Research 1.1 (2010): 13-28. Web.

[20] He, You Qiu et al. "A Study On The Sizes And Concentrations Of Gold Nanoparticles By Spectra Of Absorption, Resonance Rayleigh Scattering And Resonance Non-Linear Scattering." Spectrochimica Acta Part A:

Molecular and Biomolecular Spectroscopy 61.13-14 (2005): 2861-2866. Web.